The Cytokinin Oxidase/Dehydrogenase CKX1 Is a Membrane-Bound Protein Requiring Homooligomerization in the Endoplasmic Reticulum for Its Cellular Activity[1]

Michael C.E. Niemann,[a,2] Henriette Weber,[a,2] Tomáš Hluska,[b] Georgeta Leonte,[a] Samantha M. Anderson,[c] Ondřej Novák,[d] Alessandro Senes,[c] and Tomáš Werner[a,d,e,3]

[a]Institute of Biology/Applied Genetics, Dahlem Centre of Plant Sciences, Freie Universität Berlin, D-14195 Berlin, Germany
[b]Department of Molecular Biology, Centre of the Region Haná for Biotechnological and Agricultural Research, Palacký University, 78371 Olomouc, Czech Republic
[c]Department of Biochemistry, University of Wisconsin, Madison, Wisconsin 53706
[d]Laboratory of Growth Regulators, Centre of the Region Haná for Biotechnological and Agricultural Research, Palacký University and Institute of Experimental Botany ASCR, 78371 Olomouc, Czech Republic
[e]Institute of Plant Sciences, University of Graz, 8010 Graz, Austria

ORCID IDs: 0000-0002-1854-3949 (T.H.); 0000-0001-6114-0427 (S.M.A.); 0000-0003-3452-0154 (O.N.); 0000-0002-3807-2275 (A.S.); 0000-0001-5179-0581 (T.W.).

Degradation of the plant hormone cytokinin is controlled by cytokinin oxidase/dehydrogenase (CKX) enzymes. The molecular and cellular behavior of these proteins is still largely unknown. In this study, we show that CKX1 is a type II single-pass membrane protein that localizes predominantly to the endoplasmic reticulum (ER) in Arabidopsis (*Arabidopsis thaliana*). This indicates that this CKX isoform is a bona fide ER protein directly controlling the cytokinin, which triggers the signaling from the ER. By using various approaches, we demonstrate that CKX1 forms homodimers and homooligomers in vivo. The amino-terminal part of CKX1 was necessary and sufficient for the protein oligomerization as well as for targeting and retention in the ER. Moreover, we show that protein-protein interaction is largely facilitated by transmembrane helices and depends on a functional GxxxG-like interaction motif. Importantly, mutations rendering CKX1 monomeric interfere with its steady-state localization in the ER and cause a loss of the CKX1 biological activity by increasing its ER-associated degradation. Therefore, our study provides evidence that oligomerization is a crucial parameter regulating CKX1 biological activity and the cytokinin concentration in the ER. The work also lends strong support for the cytokinin signaling from the ER and for the functional relevance of the cytokinin pool in this compartment.

Cytokinin is a plant hormone involved in a wide range of biological processes from cell proliferation and differentiation, tissue patterning and organ initiation, to physiological responses to the environment (Werner and Schmülling, 2009; Hwang et al., 2012). Cytokinin concentrations need to be dynamically adjusted in different cell types to optimize developmental processes and growth. An important mechanism contributing to this regulation is the irreversible metabolic degradation catalyzed by cytokinin oxidase/dehydrogenase (CKX) enzymes encoded by a small gene family comprising seven members in Arabidopsis (*Arabidopsis thaliana*; Schmülling et al., 2003). Individual CKX isoforms are expressed in different tissues (Werner et al., 2003; Bartrina et al., 2011; Köllmer et al., 2014) and differ partially in their substrate specificities (Galuszka et al., 2007; Kowalska et al., 2010). It has been proposed that individual CKX proteins also control partly different cellular cytokinin pools depending on their subcellular localizations. Whereas CKX7 apparently is the only Arabidopsis isoform localized to the cytosol (Köllmer et al., 2014), CKX1 to CKX6 contain a highly hydrophobic N-terminal domain serving as a target sequence for their import to the endoplasmic reticulum (ER; Schmülling et al., 2003; Werner et al., 2003).

The ER is the entry compartment of the secretory pathway consisting of multiple organelles with distinct

[1] This work was supported by the Deutsche Forschungsgemeinschaft (WE 4325/1-1 and WE 4325/2-2), the Czech Science Foundation (GA15-22322S), the Ministry of Education, Youth, and Sports of the Czech Republic (National Program of Sustainability I, grant LO1204), National Institutes of Health grant R01GM0997522, National Science Foundation grant CHE-1415910, and the Nancy Lurie Marks Family Foundation training grant 5T15LM007359 to the CIBM Training Program.

[2] These authors contributed equally to the article.

[3] Address correspondence to tomas.werner@uni-graz.at.

The author responsible for distribution of materials integral to the findings presented in this article in accordance with the policy described in the Instructions for Authors (www.plantphysiol.org) is: Tomáš Werner (tomas.werner@uni-graz.at).

M.C.E.N., H.W., A.S., and T.W. designed experiments and analyzed the data; M.C.E.N., H.W., T.H., G.L., S.M.A., and O.N. performed experiments; T.W. wrote the article with contributions of all the authors.

www.plantphysiol.org/cgi/doi/10.1104/pp.17.00925

morphologies and functions. Secretory proteins usually enter the ER cotranslationally. Translocation of soluble proteins is directed by a cleavable N-terminal signal peptide. Integral membrane proteins possess one or more hydrophobic transmembrane (TM)-spanning regions that are inserted into the membrane of the ER. Single-pass type I membrane proteins have a cleavable signal peptide and a separate TM domain and are oriented with their N terminus in the lumen of an organelle and their C terminus in the cytoplasm. By contrast, type II membrane proteins have an uncleavable signal anchor close to the N terminus serving both as a targeting signal and as a TM helix. This type of protein exhibits an opposite topology (i.e. the C terminus faces the organellar lumen and the N terminus faces the cytosol; von Heijne and Gavel, 1988; van Anken and Braakman, 2005). Soluble and membrane cargo proteins are transported bidirectionally between organelles in membranous vesicles that are generated by cytoplasmic coat proteins (Schekman and Orci, 1996). In the biosynthetic anterograde pathway, proteins shuttle from the ER through the Golgi apparatus to reach the plasma membrane and extracellular space or vacuoles. The retrograde traffic facilitates endocytosis and the recycling of membranes and directs resident proteins back to their original compartments (Rojo and Denecke, 2008). Protein sorting into different compartments is generally mediated by sorting determinants contained within the cargo proteins themselves. These sorting determinants consist of either short conserved amino acid sequences, which are recognized by respective sorting receptors, or of physical properties such as the length and hydrophobicity of the TM span (Jürgens, 2004; De Marcos Lousa et al., 2012; Cosson et al., 2013; Gao et al., 2014; Chevalier and Chaumont, 2015).

The distribution and fate of individual CKX isoforms within the secretory system are not well understood. Some CKX isoforms, such as CKX2, were shown to be secreted from cells in heterologous yeast expression systems (Bilyeu et al., 2001; Werner et al., 2001), providing indirect evidence that these isoforms might be targeted to the apoplast in plants. This hypothesis is supported by direct localization of a CKX homolog from maize (*Zea mays*) to the apoplast (Galuszka et al., 2005). In contrast, the localization of CKX proteins to intracellular compartments of the secretory pathway has been proposed based on the localization of CKX1-GFP and CKX3-GFP reporter proteins to the ER and, occasionally, to vacuoles (Werner et al., 2003). Intriguingly, the ER localization of CKX1 has been indirectly supported by the apparent absence of hybrid and complex *N*-glycans (Niemann et al., 2015), which are synthesized on *N*-glycoproteins upon their arrival to the Golgi apparatus (von Schaewen et al., 1993).

The cytokinin signal is perceived by sensor His kinases (Inoue et al., 2001; Suzuki et al., 2001), which are localized predominantly to the ER membrane and, to a lesser extent, to the plasma membrane (Caesar et al., 2011; Lomin et al., 2011; Wulfetange et al., 2011), indicating that the steady-state cytokinin concentration in the ER lumen and apoplast might determine cellular responses to the hormone. Given the possibility that the sites of cytokinin degradation and perception might spatially overlap within the secretory system, it is essential to understand the precise distribution of CKX proteins and the underlying sorting mechanisms. Moreover, a recent study revealing the relevance of endoplasmic reticulum-associated degradation (ERAD; Römisch, 2005) for the control of CKX protein levels and plant development (Niemann et al., 2015) has demonstrated the necessity to explore molecular mechanisms controlling CKX proteins in the secretory system.

Here, we show that Arabidopsis CKX1 is an intrinsic membrane protein localized predominantly to the ER and forming homooligomeric complexes. Our data provide insights into oligomerization mechanisms mediated largely by the TM helices and indicate the functional relevance of complex formation for subcellular localization and protein stability. We propose that some CKX isoforms, including CKX1 as a case example, act as authentic ER-resident proteins to control the cytokinin homeostatic levels in the ER lumen, thereby directly regulating the signaling output from this compartment.

RESULTS

CKX1 Is a Type II Integral Membrane Protein

Our previous experimental work (Niemann et al., 2015) has suggested that, potentially, not all CKX proteins are soluble proteins, as is generally assumed. In order to directly test the solubility and possible membrane association, we focused on Arabidopsis CKX1 and prepared microsomal membranes from *Nicotiana benthamiana* leaves transiently expressing *35S:myc-CKX1* (Niemann et al., 2015). The protein gel-blot analysis showed that myc-CKX1 was detected exclusively in the 100,000*g* pellet fraction but not in the supernatant, indicating that it is either a membrane-associated protein or a soluble luminal protein (Fig. 1A). To differentiate between these possibilities, the microsomal vesicles were subjected to differential solubilization. As shown in Figure 1A, treatment with Na_2CO_3 (pH 11), which converts closed microsomal vesicles to open membrane sheets, thereby releasing the soluble luminal proteins and peripheral membrane proteins (Fujiki et al., 1982; Mothes et al., 1997), did not release myc-CKX1 from microsomal vesicles. Treatment with urea, which also extracts peripheral and luminal proteins (Schook et al., 1979; Obrdlik et al., 2000), was similarly ineffective, indicating that myc-CKX1 is not a soluble luminal protein but rather is tightly anchored within the membrane. In accord with this conclusion, myc-CKX1 could only be displaced from membranes by Triton X-100 treatment (Fig. 1A), indicating that CKX1 is a true integral membrane protein. Consistent with this experimental result, the SignalP 4.0 algorithm discriminating signal peptides from TM regions (Petersen et al., 2011) predicts the presence of an

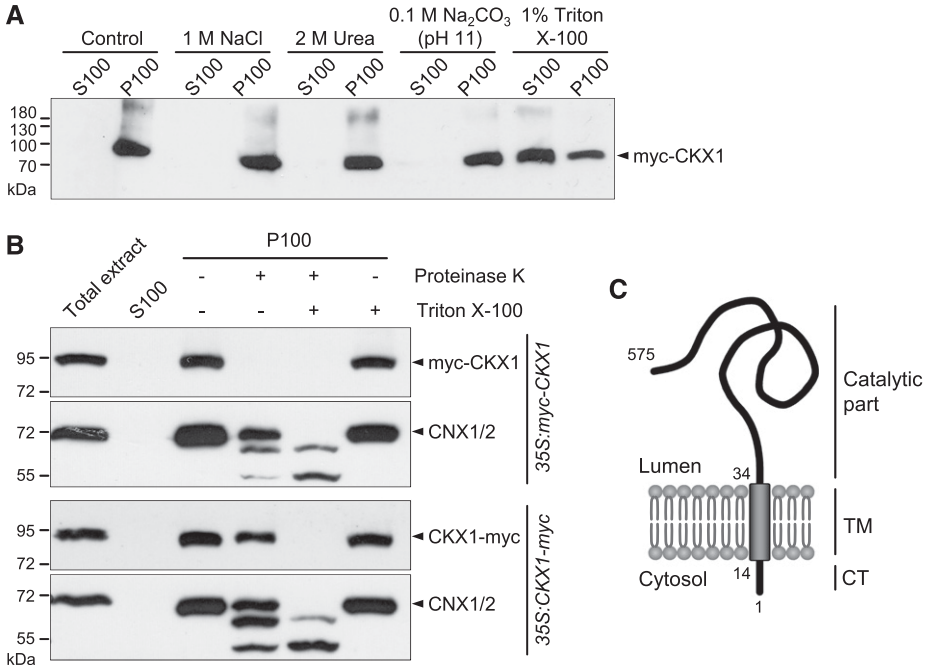

Figure 1. Membrane association and membrane topology of the myc-fused CKX1 proteins. A, Association of myc-CKX1 with membranes. Total membranes isolated from *N. benthamiana* leaves transiently expressing *35S:myc-CKX1* were incubated in homogenization buffer (control) or treated with 1 M NaCl, chaotropic agent (Urea), alkaline solution, or Triton X-100. Soluble (supernatant; S100) and insoluble (pellet; P100) membrane protein fractions were separated by recentrifugation at 100,000*g*. The proteins were resolved by SDS-PAGE and submitted to immunoblot analysis with anti-myc antibody. B, Proteinase K protection assay to reveal the membrane topology of CKX1: the C terminus of CKX1 is protected from proteinase K digestion. Microsomal membranes of *35S:myc-CKX1*- and *35S:CKX1-myc*-expressing Arabidopsis plants were incubated with proteinase K in the absence (lane 4) or presence (lane 5) of 1% Triton X-100. The samples were analyzed by SDS-PAGE and immunoblot with anti-myc antibody. Control immunoblot analysis using antibody against the luminal domain of the ER-localized, membrane-bound CALNEXIN1 and CALNEXIN2 (CNX1/2) was performed to monitor the integrity of the microsomal vesicles. C, Model of CKX1 topology in the membrane. Type II membrane protein topology included a predicted short cytosolic tail (CT), a single membrane-spanning helix (TM), and a lumen-oriented catalytic domain. Numbers indicate amino acid residues.

uncleavable signal anchor for CKX1 rather than a cleavable signal peptide (Table I). The TM-spanning region is predicted to comprise amino acid residues 14 to 34 (Table I). A similar prediction was obtained for CKX3 and CKX6, whereas the other CKX proteins with higher probability possess signal peptides (Table I).

To determine the CKX1 topology in the membrane, we performed a proteinase K protection assay with microsomal vesicles isolated from Arabidopsis plants stably expressing either the *35S:myc-CKX1* gene (Niemann et al., 2015) or CKX1 fused to a myc tag at the C terminus (*35S:CKX1-myc*). Proteinase K digestion typically results in the proteolytic removal of polypeptides that are exposed on the cytoplasmic face of microsomal vesicles. Immunoblot analysis revealed that proteinase K treatment of intact 35S:myc-CKX1 microsomes in the absence of detergent led to a complete loss of the myc signal (Fig. 1B), indicating that the N-terminally fused myc tag of the myc-CKX1 chimera was localized on the cytosolic membrane face. The proteolysis of ER chaperone proteins, CNX1/2, was used as a positive control in this proteolysis protection assay. Calnexins are conserved single-pass membrane proteins consisting of a large luminal domain and short tail facing the cytosol (Huang et al., 1993). Consistent with their topology, immunoblot analysis of proteinase K-treated microsomes showed that CNX1/2 were largely protected from the proteolysis, indicating high integrity of the microsomal membrane preparations. In contrast to myc-CKX1, the CKX1-myc fusion protein in microsomes isolated from *35S:CKX1-myc*-expressing plants was largely protected from proteinase K activity and, similar to CNX1/2, was fully susceptible to proteolysis only in the presence of the detergent, indicating that the myc-tagged C terminus of CKX1 was localized in the microsomal lumen. Together, our results show that CKX1 is a typical type II membrane protein with topology consisting of a short cytoplasmic tail, a single TM region, and a large, luminally oriented, C-terminal catalytic domain (Fig. 1C).

CKX1 Forms Homooligomeric Complexes

Immunoblot analyses of protein extracts from *35S:CKX1* plants repeatedly showed that CKX1 partly runs

Table I. *Bioinformatic prediction to discriminate signal peptide and signal anchor sequences in Arabidopsis CKX proteins*

Protein	SignalP 4.1 (D-Score)[a]	Signal Peptide (P)/Signal Anchor (A)	TM Domain (Residues)[b]
CKX1 (At2g41510.1)	0.302	A	14–34
CKX2 (At2g19500.1)	0.738	P	–
CKX3 (At5g56970.1)	0.332	A	9–29
CKX4 (At4g29740.1)	0.683	P	–
CKX5[c] (At1g75450.1)	0.729	P	–
CKX5[c] (At1g75450.2)	0.775	P	–
CKX6 (At3g63440.1)	0.261	A	16–36

[a]Signal peptide/anchor prediction was performed with SignalP 4.1 (http://www.cbs.dtu.dk/services/SignalP/). D-score indicates the likelihood of signal peptide cleavage. [b]TM domains were predicted by ConPred_v2 at the Aramemnon database (Schwacke et al., 2003). [c]Different translation starts resulting in different N termini are predicted in TAIR (http://www.arabidopsis.org/).

as an SDS-resistant complex of higher molecular mass on a reducing SDS-PAGE gel (Fig. 1A), which indicates potential tight interactions with other proteins or protein homooligomerization. To analyze specifically whether CKX1 can homooligomerize, GFP-CKX1 and myc-CKX1 fusion proteins were transiently coexpressed in *N. benthamiana* leaves, and total protein extracts were used for coimmunoprecipitation (Co-IP) assay with an anti-GFP antibody. As shown in Figure 2A, myc-CKX1 was detected robustly in the GFP-CKX1 immunocomplex, but it did not coimmunoprecipitate with GFP alone, strongly supporting the notion of CKX1 homodimerization in vivo. Interestingly, Figure 2A shows that, in contrast to the input samples, the myc-CKX1 signal of high molecular mass was the most prevalent in the Co-IP fraction. This suggests the formation of a higher order oligomer that was not fully resolved under SDS-PAGE conditions.

To examine the CKX1 oligomerization in more detail, we subjected protein extracts from *N. benthamiana* expressing myc-CKX1 to size exclusion chromatography (SEC; Fig. 2, B–D). Given the strong membrane association of myc-CKX1 (Fig. 1), the membrane proteins were solubilized with the nonionic detergent DDM, and the detergent was included in the chromatography buffer during SEC fractionation at a concentration above the critical micelle concentration. Solubilization of membranes by detergents converts intrinsic membrane proteins into complexes composed of protein, lipid, and detergent. The micelle size of the detergent used contributes to the final molecular mass of a given complex, thus influencing the elution volume during SEC (Kunji et al., 2008). Three major peaks of different apparent molecular sizes containing myc-CKX1 were detected. One myc-CKX1 peak eluted late, with an elution volume of 62 to 63 mL corresponding to an apparent molecular mass of ~130 to 140 kD (Fig. 2C). The average molecular mass of a DDM micelle is ~50 kD (Rögner, 2000) and the apparent molecular size of the myc-CKX1 monomer is ~90 kD, as deduced from the protein migration on the SDS-PAGE gel (Fig. 2A). Thus, the myc-CKX1 peak with an apparent size of ~130 to 140 kD corresponds to the myc-CKX1 monomer. The second myc-CKX1 peak eluted with a retention volume of 55 to 56 mL corresponding to an apparent molecular mass range of 215 to 230 kD and most probably represented the myc-CKX1 homodimeric form. The third peak, with a retention volume of 43 to 44 mL and apparent mass of around 470 to 510 kD, represented a higher oligomeric form of myc-CKX1 protein. Interestingly, the immunoblot analysis revealed that the apparent myc-CKX1 homodimer and higher oligomer were partly stable under our SDS-PAGE conditions. Intriguingly, when the SEC experiment was performed under reducing conditions with 5 mM β-mercaptoethanol included in the chromatography buffer, similar results were obtained and the different oligomeric forms of myc-CKX1 were detected (Supplemental Fig. S2).

To test CKX1 oligomerization independently and determine whether the protein-protein interaction also can occur in planta, oligomerization was tested using the optimized single vector bimolecular fluorescence complementation (BiFC) system, which utilizes monomeric Venus split at residue 210 (Gookin and Assmann, 2014). For this, *CKX1* was cloned in two expression cassettes of the double open reading frame expression vector pDOE-08, and by this, the N termini of two individual CKX1 proteins were fused to the N- and C-proximal halves of Venus (NVen and CVen, respectively). To monitor the nonspecific assembly of NVen and CVen, the parent vector expressing NVen-CKX1 and unfused CVen was used as a control. The vector used also contains an integrated Golgi-localized mTurquoise2 marker (Golgi-mTq2) for the specific identification of transformed cells. We performed transient transformations of *N. benthamiana* leaves and examined the fluorescence by confocal laser scanning microscopy. We identified expressing epidermal cells by monitoring the Golgi-mTq2 fluorescence, and, as illustrated in Figure 3A, all transformed cells showed very strong Venus fluorescence, indicating BiFC

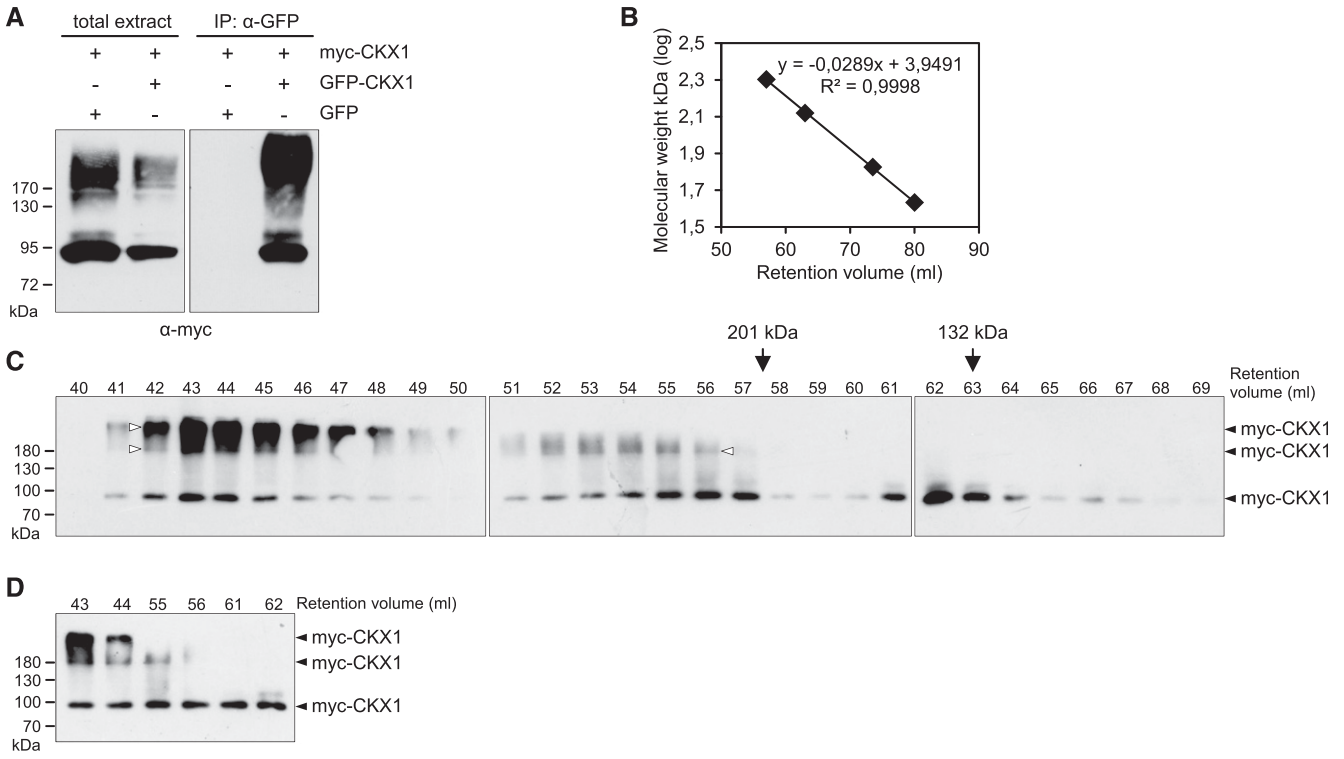

Figure 2. Analysis of CKX1 oligomerization. A, In vivo oligomerization of CKX1 detected by Co-IP assay. The myc-CKX1 protein was transiently coexpressed with GFP-CKX1 or GFP in *N. benthamiana*, and the protein extracts were used for immunoprecipitations (IP) with anti-GFP antibody followed by immunoblot detection with anti-myc antibody. The left gel shows the input (10 μg of the crude extract used for Co-IP assay); the right gel shows the pellet fractions from the Co-IP assays. The input control for GFP-CKX1 and GFP is shown in Supplemental Figure S1. B to D, SEC analysis of CKX1 complex formation. B, For the column calibration, the standard linear regression curve was generated by plotting the log of the molecular mass of calibration proteins against their retention volumes: BSA trimer (201 kD; 57.5 min), BSA dimer (132 kD; 63 min), BSA monomer (67 kD; 73.5 min), and ovalbumin (43 kD; 80 min). C, Microsomal membranes isolated from *N. benthamiana* leaves transiently expressing *35S:myc-CKX1* were solubilized with 1% *n*-dodecyl-β-D-maltoside (DDM) and subjected to SEC on a column equilibrated with 0.05% DDM, 50 mM Tris-HCl, pH 7.5, 10% glycerol, and 150 mM NaCl. Eluted fractions were analyzed by SDS-PAGE and immunoblot with anti-myc antibody. Arrows indicate peak elutions of molecular mass markers (BSA trimer and dimer). White arrowheads indicate the resistant dimeric and higher oligomeric myc-CKX1 forms. D, Six elution fractions from the experiment shown in C were reanalyzed in parallel on one western blot.

between NVen-CKX1 and CVen-CKX1. By contrast, no BiFC was detected when NVen-CKX1 was coexpressed with the untagged CVen fragment, although the analyzed cells displayed strong Golgi-mTq2 fluorescence (Fig. 3B), thus proving to be a genuine negative control. From these results, we conclude that CKX1 can assemble into a homooligomeric complex in planta.

CKX1 Is an ER-Resident Protein

Further detailed microscopic analysis showed that the NVen-CKX1/CVen-CKX1 BiFC signal was distributed in a reticular pattern characteristic of the cortical ER network (Fig. 3C). To verify this, we cotransformed the CKX1-BiFC construct with an ER marker protein (Lerich et al., 2011). The colocalization of the BiFC and ER marker signals indicated that the putative CKX1 homodimer localizes to the ER. This localization would be only partially consistent with the previously published data, which have shown that CKX1-GFP localized largely to the ER but occasionally also to the vacuole when expressed stably in Arabidopsis under the control of the 35S promoter (Werner et al., 2003). These earlier experiments, however, might not have been fully conclusive, due to possible overexpression artifacts (Werner et al., 2003). Indeed, Niemann et al. (2015) recently showed that CKX1 apparently does not contain complex *N*-glycans, which is consistent with the idea that CKX1 could be an ER-resident protein. To examine the CKX1 subcellular localization and avoid strong overexpression effects, we tagged CKX1 with GFP at the N terminus (recapitulating the topology of the chimeric proteins in the BiFC assay), expressed the fusion protein transiently in *N. benthamiana* leaves, and performed confocal imaging at early time points after infiltration. As shown in Figure 4A, early after infiltration, GFP-CKX1 was localized exclusively to the ER in

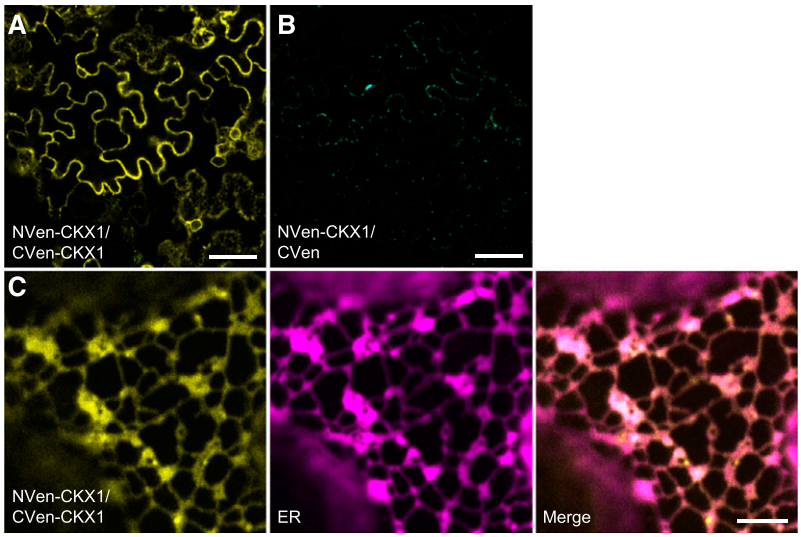

Figure 3. CKX1 homodimerizes in a BiFC assay. A, Confocal microscopy analysis of BiFC in *N. benthamiana* epidermal leaf cells reveals interaction between NVen-CKX1 and CVen-CKX1, as apparent from the reconstitution of the Venus-derived fluorescence (yellow). The microscopy was performed 2 d after infiltration (DAI). B, The NVen-CKX1/CVen parent vector shows no background BiFC signal 2 DAI. Successful transformation is evident from the cyan mTq2 signal in the Golgi. No BiFC signal was observed even after prolonged incubation (3 DAI). Images in A and B were captured using identical confocal settings. C, NVen-CKX1/CVen-CKX1 BiFC fluorescence signal localizes predominantly to the ER. Yellow, Venus BiFC; magenta, RFP-p24. Bars = 50 μm (A and B) and 5 μm (C).

cells moderately expressing the fusion protein. In cells with higher expression levels, the GFP-CKX1 fluorescence signal also was localized to bright puncta of varying sizes (Supplemental Fig. S3). However, a similar shift of the fluorescence signal from the ER network into punctate structures also was often observed for the ER membrane marker RFP-p24 (Lerich et al., 2011) when expressed to higher levels (Supplemental Fig. S3A), which suggests either an aberrant protein localization due to exceeded ER retention capacity or general changes in the ER morphology. The latter assumption was further supported by a frequent colocalization of the strongly expressed GFP-CKX1 with the tobacco mosaic virus movement protein (MP-RFP; Sambade et al., 2008; Supplemental Fig. S3B), marking ER-associated inclusions whose formation is associated with rearrangements of the ER membrane.

To analyze the possibility that the N-terminal GFP fusion masked an important targeting signal in the cytoplasmic tail of CKX1, we also transiently expressed CKX1 fused C-terminally to GFP under the control of the *35S* promoter (CKX1-GFP). Compared with the CKX1-GFP construct reported previously (Werner et al., 2003), this new chimeric protein includes a short linker to provide flexibility between the fused proteins (Miyawaki et al., 2003). Figure 4B shows that the fusion protein was localized predominantly to the ER with additional GFP signal associated with small endogenous, motile compartments (arrowheads). We first tested whether the punctate signal might represent endoplasmic reticulum export sites (ERES; Hanton et al., 2006) by coexpression of the ERES marker protein YFP-Sec24 (Stefano et al., 2006); however, we observed no colocalization (Fig. 4C). Next, we analyzed colocalization with markers for some of the well-defined post-ER compartments. The cis-Golgi marker ERD2-YFP (Brandizzi et al., 2002) did not colocalize with the punctate CKX1-GFP signal (Fig. 4D). CKX1-GFP also did not colocalize with the trans-Golgi network/early endosome marker mCherry-SYP61 (Uemura et al., 2004; Gu and Innes, 2011; Fig. 4E). Intriguingly, upon coexpression with ARA6-mCherry, which labels prevacuolar compartments/late endosomes (Ueda et al., 2001; Gu and Innes, 2012), we observed that the punctate CKX1-GFP signal mostly localized in very close proximity to the ARA6-mCherry signal and occasionally colocalized with it (Fig. 4F). From the above experiments, we conclude that, similar to GFP-CKX1, the CKX1-GFP protein is localized mainly to the ER and to its closely associated punctate structures of not fully resolved nature.

The N-Terminal Part of CKX1 Is Required and Sufficient for Homooligomerization and Targeting to the ER

Interestingly, we observed no homodimerization in a yeast two-hybrid assay when truncated CKX1 protein without N-terminal signal anchor sequence ($CKX1^{35\text{-}575}$) was used, although this mutant form was capable of interacting with other proteins in yeast (H. Weber, unpublished data). This indicates that the CKX1 N terminus might be relevant for the homooligomerization. In order to test this hypothesis, we generated a chimeric

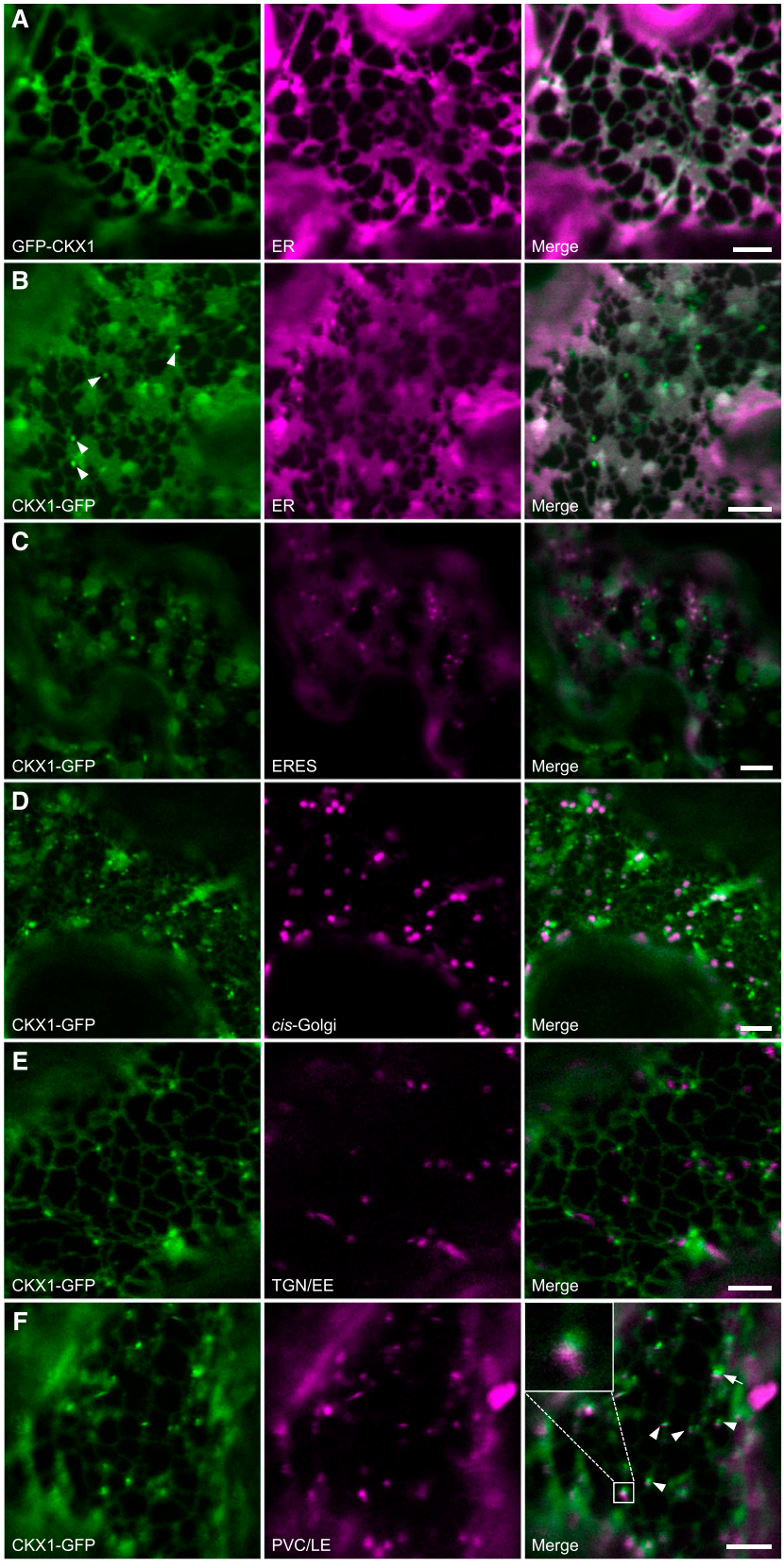

Figure 4. CKX1 fusion proteins to GFP localize predominantly to the ER. Confocal microscopy analysis was performed on *N. benthamiana* leaf epidermal cells coexpressing different GFP-fused CKX1 chimeric proteins (left column; green) and the indicated organelle markers (middle column; magenta). A, GFP-CKX1 colocalizes with the ER marker protein RFP-p24 when expressed 1 d after infiltration (DAI). B to E, CKX1-GFP largely colocalizes with the ER marker protein (B) and shows additional localization in small punctate structures (arrowheads), which are distinct from ERES labeled by YFP-Sec24 (C), Golgi bodies labeled by ERD2-YFP (D), and trans-Golgi network/early endosome (TGN/EE) labeled by mCherry-SYP61 (E). F, CKX1-GFP signal localizes mostly close to prevacuolar compartments/late endosomes (PVC/LE) labeled by ARA6-mCherry (arrowheads and magnified in inset). Occasionally, CKX1-GFP and ARA6-mCherry signals overlapped (arrow). The microscopy was performed 2 DAI. Bars = 5 μm.

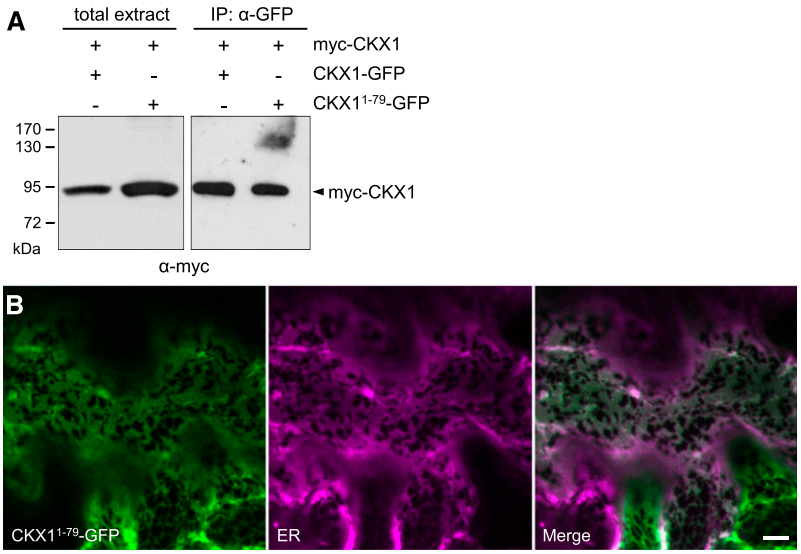

Figure 5. The CKX1 N terminus directs the homooligomerization and targeting to the ER. A, Co-IP assay for the detection of homooligomerization mediated by the CKX1$^{1-79}$ N-terminal fragment. The myc-CKX1 protein was coexpressed transiently with CKX1$^{1-79}$-GFP or CKX1-GFP in *N. benthamiana*, and the protein extracts were used for immunoprecipitations (IP) with anti-GFP antibody followed by immunoblot detection with anti-myc antibody. The left gel shows the input (10 μg of the crude extract used for Co-IP assay); the right gel shows the pellet fractions from the Co-IP assays. The input control for CKX1$^{1-79}$-GFP and CKX1-GFP is shown in Supplemental Figure S4. B, Confocal microscopy analysis of *N. benthamiana* leaf epidermal cells coexpressing CKX1$^{1-79}$-GFP (green) with the ER marker RFP-p24 (magenta). The microscopy was performed 2 DAI. Bars = 5 μm.

reporter construct consisting of the first 79 N-terminal amino acid residues (comprising the cytoplasmic tail, TM domain, and putative stem region) of CKX1 fused to GFP (CKX1$^{1-79}$-GFP). To test the capacity of this short N-terminal peptide to mediate the homooligomerization, CKX1$^{1-79}$-GFP was coexpressed transiently together with myc-CKX1 in *N. benthamiana* leaves and used as bait in Co-IP experiments. Immunoblot analysis revealed that myc-CKX1 copurified robustly with CKX1$^{1-79}$-GFP (Fig. 5A; Supplemental Fig. S4). In parallel, we performed a control Co-IP assay with the full-length CKX1 protein tagged C terminally with GFP (CKX1-GFP). Interestingly, the quantity of copurified myc-CKX1 was comparable to that of CKX1$^{1-79}$-GFP (Fig. 5A), suggesting that the examined N-terminal region of CKX1 is primarily responsible for homooligomeric complex formation.

Next, we questioned the role of the CKX1 N terminus in directing the subcellular localization of the protein and compared the subcellular localization of CKX1$^{1-79}$-GFP with that of the full-length reporter CKX1-GFP. Transient expression and confocal imaging of CKX1$^{1-79}$-GFP revealed very similar subcellular localization comparable to that of the full-length reporter CKX1-GFP (Fig. 5B), suggesting that the N-terminal peptide is sufficient for the targeting and retrieval to the ER.

The CKX1 TM Domain Is Required for Protein Homooligomerization

Showing the relevance of the N-terminal part of CKX1 for homooligomerization and subcellular localization, we further aimed to delimitate the functional motifs relevant for these processes. Several reports have shown that TM helices of type II membrane proteins can mediate protein oligomerization involving different interaction mechanisms (Tu and Banfield, 2010). CKX1 contains a potential GxxxG-like interaction motif (SxxxG) formed by residues Ser-27 and Gly-31 (Fig. 6A). GxxxG-like motifs consist of small amino acids (Gly, Ala, and Ser) arranged to form GxxxG (where x represents any amino acid) and GxxxG-like patterns (Russ and Engelman, 2000; Senes et al., 2000). These interaction motifs often are found at the interface of GAS_{right} dimers, a frequently occurring TM association motif (Walters and DeGrado, 2006) characterized by the close proximity of the two TM helices and the formation of characteristic networks of carbon hydrogen bonds (Senes et al., 2001). We employed the computational structure prediction program CATM (Mueller et al., 2014; Anderson et al., 2017) to investigate whether the TM helices of CKX1 proteins may associate by forming a GAS_{right} dimer.

As shown in Figure 6A, CATM predicts a plausible GAS_{right} dimer for the TM sequence of CKX1. The resulting model is characterized by favorable complementary packing and mediated by the SxxxG motif. It should be noted that the software assumes that the TM domain is in regular helical conformation. The sequence of CKX1 contains a Pro residue at position 30, an amino acid that could potentially kink the helices, even though Pro also is compatible with straight or nearly straight conformation in TM helices (Senes et al., 2004). The Pro residue occurs on the opposite face of the dimeric

contact; thus, it does not participate in the predicted interface. The amino acids that are involved at the dimer interface are highlighted in the sequence in Figure 6A.

Computational mutational analysis indicated that introduction of the large Ile in place of the small amino acids of the SxxxG motif (Ser-27Ile and Gly-31Ile) would create significant steric clashes in the model; thus, it should prevent any dimerization mediated by the predicted association interface (Supplemental Fig. S6). To test the prediction, we introduced two Ile residues (Ser-27Ile and Gly-31Ile) in the full-length CKX1 protein and analyzed the homodimerization ability of the resulting mutant protein (CKX1) in a BiFC assay. Compared with the nonmutagenized control, BiFC between NVen-CKX1 and CVen-CKX1 was reduced severely (Fig. 6, B and C), suggesting that the interaction was mediated largely by the TM domain and that the identified residues are functionally relevant. Importantly, CKX1-GFP was glycosylated in a similar fashion to the control, and the mutant protein was detected exclusively in the membrane protein fraction (Supplemental Fig. S5), indicating that the introduced mutations in the TM region neither altered the capacity of the signal anchor to translocate the protein into the ER nor compromised the general helix structure and anchoring to the membrane.

CKX1 Oligomerization Is Indispensable for Its Biological Activity

We further examined whether the altered ability of CKX1-GFP to oligomerize affects the cellular behavior and biological activity of the protein. Confocal microscopy showed that, in comparison with the CKX1-GFP control (Fig. 4B), the fluorescence signal of CKX1-GFP was completely absent from the ER and accumulated in vesicles and vesicular aggregates of varying sizes (Fig. 6D). In addition, the overall CKX1-GFP fluorescence signal was reduced greatly in comparison with that of CKX1-GFP, together suggesting that the TM-mediated oligomerization regulates CKX1 retention/localization to the ER and/or contributes to the control of protein abundance in the ER. To address the biological relevance of the CKX1 oligomerization, we analyzed Arabidopsis plants stably expressing *CKX1-GFP* or *CKX1-GFP* under the control of the 35S promoter. The shoots of plants expressing the *35S:CKX1-GFP* transgene displayed strong phenotypic changes typical for cytokinin deficiency (Fig. 7A; Werner et al., 2003; Holst et al., 2011), with a frequency of 45% among T1 plants. In comparison, we only detected very subtle phenotypic alterations among 90 T1 individuals transformed with the *35S:CKX1-GFP* construct. To rule out the possibility that the observed differences were due to different transgene expression levels, we identified homozygous lines with comparable transcript levels of the respective transgene (Fig. 7C; Supplemental Fig. S7). This analysis confirmed that the strong cytokinin deficiency phenotype was associated only with the expression of the *35S:CKX1-GFP*, but not the *35S:CKX1-GFP*, transgene (Fig. 7, A and B). Moreover, immunoblot analysis revealed that the levels of the CKX1-GFP protein were strongly diminished in comparison with CKX1-GFP (Fig. 7D; Supplemental Fig. S7), which was consistent with the absence of strong phenotypical changes in plants expressing the mutant protein. In line with this, direct determination of endogenous cytokinins revealed that their levels were significantly weaker in *35S:CKX1-GFP* lines in comparison with plants expressing the nonmutated *35S:CKX1-GFP* construct (Fig. 7E; Supplemental Fig. S7).

It was shown previously that several secretory CKX proteins are regulated by the ERAD pathway (Niemann et al., 2015). Therefore, we reasoned that the low levels of the oligomerization-deficient CKX1-GFP protein variant could be due to enhanced ERAD. To test this assumption, we analyzed CKX1-GFP levels upon treatment with Eeyarestatin I (EerI) and Kifunensin (Kif), which are specific inhibitors of the ERAD pathway (Tokunaga et al., 2000; Fiebiger et al., 2004; Wang et al., 2010). Figure 7D shows that the CKX1-GFP levels increased significantly upon both treatments. Similarly, CKX1-GFP levels were enhanced significantly by the proteasome inhibitor MG132. Together, these results suggest that the lower CKX1-GFP steady-state levels were caused by increased ERAD and that the CKX1 oligomerization is an important factor regulating its stability in the ER.

DISCUSSION

Taking CKX1 from Arabidopsis as a case example, this study draws attention to several new molecular and cellular aspects of CKX-mediated cytokinin degradation and provides results that are relevant for better understanding of the functional modality of this metabolic pathway in controlling cytokinin activity in plants.

First, we demonstrated that CKX1 is not a soluble protein but an integral single-pass membrane protein with a type II architecture comprising a short N-terminal cytoplasmic tail, a TM helix, and a luminally oriented catalytic domain. A similar topology is typical for proteins such as Golgi- and ER-resident glycosyltransferases and glycosidases (Tu and Banfield, 2010). As signal peptides and N-terminal TM helices of the secretory pathway proteins generally are difficult to discriminate (Petersen et al., 2011), the possible membrane association of CKX proteins has been neglected previously (Schmülling et al., 2003) and clearly needs to be determined experimentally for individual CKX isoforms. Several CKX proteins have been shown convincingly to be soluble proteins containing cleavable signal peptides (Houba-Hérin et al., 1999; Galuszka et al., 2005), which, together with our results, suggests that two different subtypes of CKX isoforms, soluble and membrane bound, operate in the secretory system.

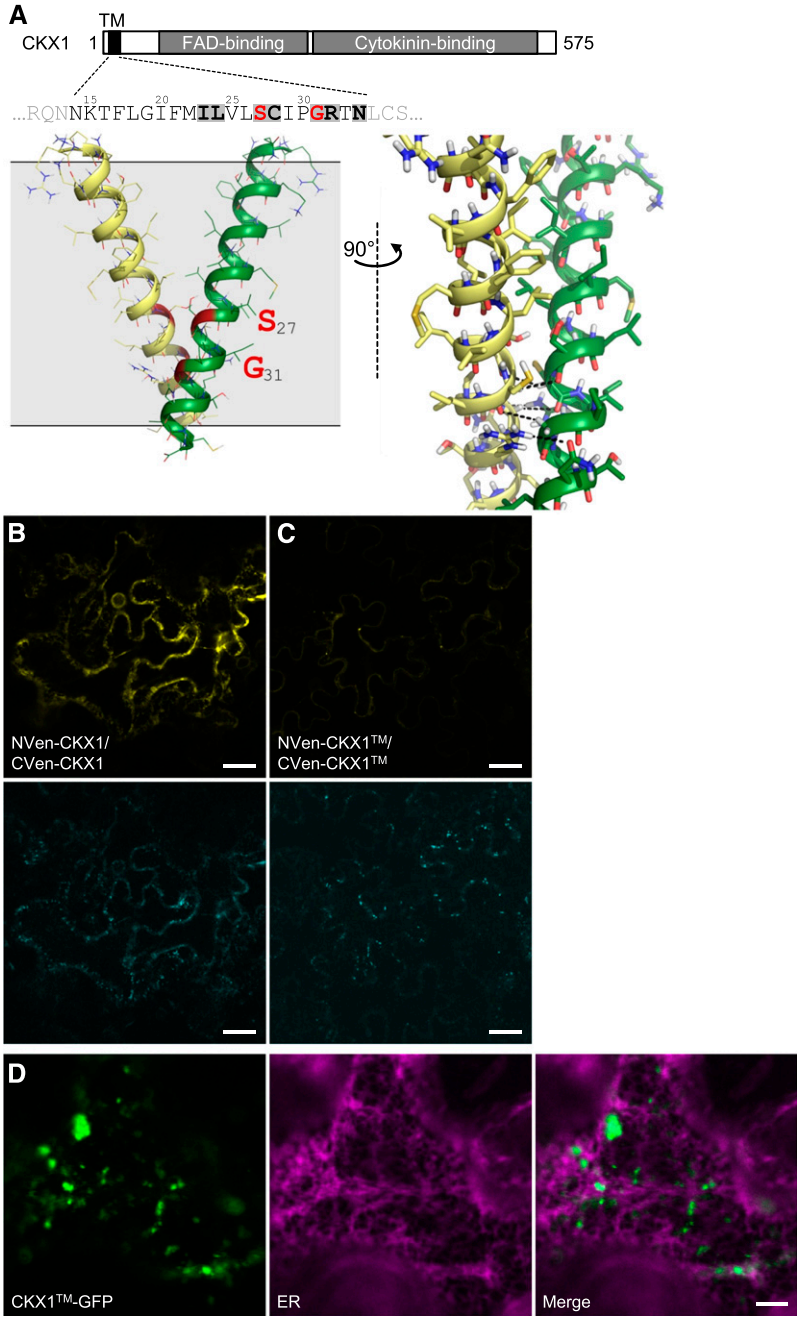

Figure 6. The CKX1 TM domain mediates the protein homooligomerization and ER retention. A, Structural model of the CKX1 TM dimer predicted by CATM. From left to right, ribbon representation of the entire TM helix (front view) and detail of the interface (side view). CATM predicts a well-packed interface mediated by the amino acids highlighted in the sequence. The SxxxG sequence pattern (marked in red) allows the backbones to come into close contact at the crossing point, enabling the formation of networks of interhelical hydrogen bonds (dashed lines) between Cα-H donors and carbonyl oxygen acceptors. Additionally, an interhelical hydrogen bond between the side chains of Arg-32 and Asn-34 also is observed. B and C, Confocal microscopy analysis of BiFC in *N. benthamiana* epidermal leaf cells reveals strongly reduced interaction between NVen-CKX1 and CVen-CKX1 (C) in comparison with the interaction of NVen-CKX1 and CVen-CKX1 (B), as apparent from the reconstitution of the Venus-derived fluorescence (yellow; top images). Comparable expression levels are apparent from the activity of the control gene Golgi-mTq2 (cyan; bottom images). The microscopy was performed 2 d after infiltration (DAI). Identical confocal settings were used to capture respective images in B and C. D, Confocal microscopy analysis of *N. benthamiana* leaf epidermal cells coexpressing CKX1-GFP (green) with the ER marker RFP-p24 (magenta). The microscopy was performed 2 DAI. Bars = 25 μm (B and C) and 5 μm (D).

Along with the difference in this basic protein feature, different cellular behavior of the individual CKX isoforms can be expected as, for example, different sorting mechanisms for soluble and membrane proteins operate in the secretory pathway. Unlike for soluble proteins, sorting of membrane proteins is additionally determined by motifs located in their cytosolic domains and by the structure of the TM domain (Brandizzi et al., 2002; Gao et al., 2014). It is well established that the default destination for soluble proteins lacking positive sorting information is the apoplast (Rojo and Denecke, 2008). Indeed, several CKX isoforms shown to be soluble or having strongly predicted signal peptides have been demonstrated to be secreted to the apoplast (Houba-Hérin et al., 1999; Bilyeu et al., 2001; Galuszka et al., 2005). These findings correlate with the fact that all putative soluble CKX proteins lack obvious sorting determinants, such as the (H/K)DEL ER retention signal. Thus, it appears that soluble CKX isoforms may generally follow the default secretory route to the apoplast. In contrast, CKX1, defined in this work as a prototypic membrane-bound CKX isoform, localized predominantly to the ER. CKX1 retention in the ER is well consistent with its apparent modification by high-Man *N*-glycans (Niemann et al., 2015). This finding is highly relevant because recent reports have revealed that AHK cytokinin sensor His kinases are localized predominantly in the ER (Caesar et al., 2011; Lomin et al., 2011; Wulfetange et al., 2011). Hence, CKX1, as an authentic ER protein, presumably coincides with the ER-localized AHK proteins and controls cytokinin concentrations directly perceived by the hormone receptors in the ER lumen. This active control of the cytokinin pool in the ER by CKX lends more support to the functional relevance of cytokinin receptor-mediated signaling from this cellular compartment.

Evidence regarding CKX1 localization beyond the ER is ambiguous. For example, prolonged expression of GFP-CKX1 caused, in addition to ER localization, the accumulation of GFP signal in larger bodies that coincide with ER-associated inclusions formed, for example, upon the expression of MP-RFP (Sambade et al., 2008). GFP-CKX1 signals in these structures, therefore, may reflect changes in ER structure that can be caused by strong, transient overexpression of an ER-resident protein (Niehl et al., 2012; Supplemental Fig. S3A) rather than by the normal cellular distribution of GFP-CKX1. Additionally, in the case of the C-terminal CKX1-GFP fusion, the predominant ER signal was accompanied by localization to very small puncta, which often were positioned in direct proximity of prevacuolar compartments/late endosomes labeled by ARA6-mCherry. However, these showed only limited colocalization. The identity of these CKX1-GFP-labeled structures will require further clarification. Importantly, both analyzed CKX1 fusion proteins were not detected in the vacuole. Together, the analysis does not support our previous hypothesis that CKX1 might be actively targeted to the lytic vacuole (Werner et al., 2003). It is possible that the occasional vacuolar targeting observed previously (Werner et al., 2003) was an overexpression artifact due to saturated ER retention capacity. CKX1-GFP escaping ER retention mechanisms might passively reach the vacuole, which has been discussed as the default compartment for some membrane proteins (Barrieu and Chrispeels, 1999; Langhans et al., 2008). Accordingly, although we showed in this study that CKX1 is bound exclusively to membrane, the CKX1-GFP signal reported by Werner et al. (2003) did not label the tonoplast but the vacuolar lumen, which indicates the formation of a soluble degradation product. Taken together, there is currently no clear experimental evidence supporting the function of CKX proteins in the vacuole. However, we note that cytokinin has been detected in vacuoles (Fusseder and Ziegler, 1988; Kiran et al., 2012; Jiskrová et al., 2016), but its biological significance in this organelle remains obscure.

A surprising outcome of our study is that CKX1 forms homodimeric and oligomeric complexes in vivo. Most interestingly, complex formation was mediated mainly by a strong interaction between the TM domains. Oligomerization of the TM helices of bitopic membrane proteins can be important for the structural assembly of stable protein complexes as well as play functional roles when association or conformational changes are critical for modulating signaling and regulation (Moore et al., 2008). Classic examples are the receptor Tyr kinase and cytokine receptor families of type I membrane proteins, for which dimerization and structural rearrangement involving the TM region play critical roles in activation (Li and Hristova, 2006; Maruyama, 2015). For animal type II membrane proteins, including several Golgi glycosyltransferases, it was shown previously that protein oligomerization can be determined by the luminal juxtamembrane region and/or the TM-spanning region (Tu and Banfield, 2010).

A variety of physical forces have been implicated in the promotion of TM helix interactions (Senes et al., 2004; Li et al., 2012), from van der Waals packing (MacKenzie et al., 1997) to hydrogen bonding between polar amino acids (Choma et al., 2000; Zhou et al., 2000) and aromatic π-π and cation-π interactions (Johnson et al., 2007). A particularly important class of TM helix interaction motifs is the GAS_{right} dimer, which is stabilized by unusual networks of hydrogen bonds that are formed by Cα-H donors and backbone carbonyl oxygen acceptors on the opposite helix (Cα-H•••O=C bonds; Senes et al., 2001). The signature sequence pattern of GAS_{right} is the presence of small residues (Gly, Ala, and Ser) arranged in motifs such as GxxxG or variants thereof that facilitate close interhelical contact and carbon-hydrogen bond formation between TM helices (Mueller et al., 2014). The mutation and Co-IP analyses presented in this work showed that the identified GxxxG-like motif (SxxxG) in the TM domain of CKX1 is largely required for CKX1 homooligomerization. Currently, little is known about GxxxG-mediated protein-protein interactions and their functions in

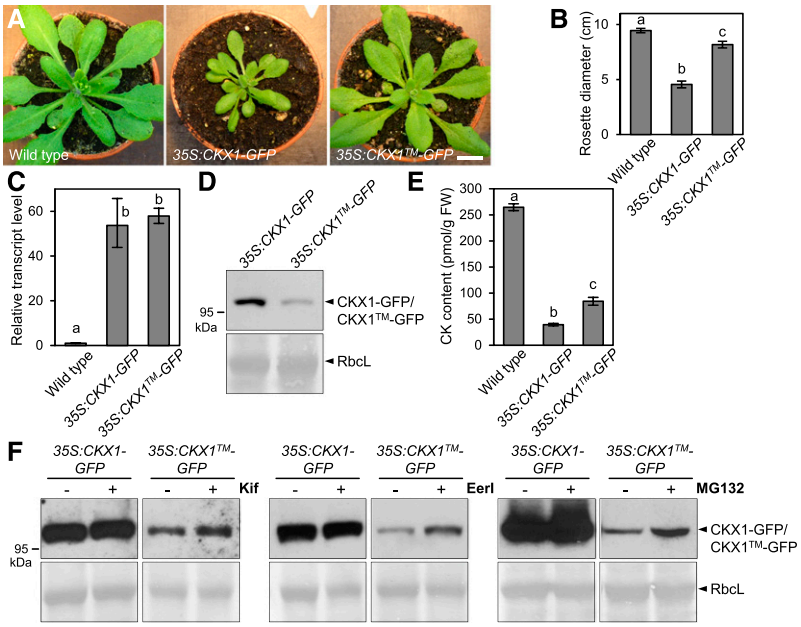

Figure 7. TM-mediated CKX1 homooligomerization regulates protein stability. A, Shoot phenotypes of the soil-grown wild-type control and plants expressing *35S:CKX1-GFP* (line 1) and *35S:CKX1-GFP* (line 14) 4 weeks after germination. Homozygous T4 plants are shown. Bar = 1 cm. B, Rosette diameters of the plants shown in A. Values are means ± SD ($n \geq 5$). C and D, Comparison of the *CKX1* transcript levels (C) and the protein abundances (D) in shoots of the *35:CKX1-GFP* and *35:CKX1-GFP* plants shown in A. Transcript levels were determined by quantitative real-time PCR. Means ± SD ($n = 4$) are shown in C. For the protein abundance analysis, 50 μg of the crude protein extracts was analyzed by immunoblot using anti-GFP antibody. Coomassie Blue staining of Rubisco large subunit (RbcL) was used as a loading control in D. E, Total cytokinin (CK) contents of the 3-week-old plants shown in A. Means ± SD ($n = 3$) are shown. FW, Fresh weight. F, Analysis of the effects of the ERAD inhibitors EerI and Kif, and of the proteasome inhibitor MG132, on CKX1-GFP and CKX1-GFP protein abundances. Arabidopsis seedlings grown in liquid cultures for 7 d were treated for 24 h with 50 μM Kif or 20 μM EerI and for 9 h with 100 mM MG132. Proteins were analyzed as described in D. In B, C, and E, different letters indicate statistically significant differences (Student's *t* test, $P < 0.05$).

plants. A TM domain containing a GxxxG motif has been reported to occur in many receptor-like kinases and receptor-like proteins mediating plant immune responses (Fritz-Laylin et al., 2005), but only two studies have addressed the function of the GxxxG motif in protein-protein interactions and signaling responses to pathogens (Zhang et al., 2010; Bi et al., 2016). In addition to dimerization, our SEC fractionations also suggested higher order oligomerization of CKX1, which is in accord with several previous reports describing the assembly of GxxxG dimers into higher oligomeric complexes (Dews and MacKenzie, 2007; Xu et al., 2007; Hoang et al., 2015; Kwon et al., 2015). Although the underlying assembly mechanisms are mostly unclear, they may involve TM domain interactions as well as interfaces in the soluble domain.

It will be important to understand whether the described protein features are conserved among CKX homologs. Our sequence analysis revealed only a related AxxxA motif (Gimpelev et al., 2004) in the TM domain of CKX6, indicating that the sequence of TM domains is not conserved and that the SxxxG motif is unique to CKX1. However, given that TM domains do not need to contain specific sequence motifs to oligomerize (Moore et al., 2008), it is currently not possible to conclude whether oligomerization is a shared mechanism in the CKX family, and individual proteins will need to be analyzed experimentally in the future.

Ultimately, it is important to understand the significance of CKX1 homooligomerization for its cellular activity. One possibility is that the CKX1 oligomeric state and its enzymatic activity would be coupled. Examples of such a structure-activity relation for type II membrane proteins are known (Chung et al., 2010; Tu and Banfield, 2010). However, heterologous expression of a chimeric CKX1 protein with the N terminus replaced by a cleavable yeast secretion signal yielded a relatively high enzyme activity preparation (Kowalska et al., 2010), suggesting that the TM-mediated oligomerization may not be required for CKX1 enzyme activity per se. Further experiments are still needed to test this possibility more rigorously. In contrast, our analysis demonstrated that mutations rendering CKX1 monomeric cause (1) a loss of its ER localization, resulting in an unspecified cellular redistribution, and (2) a reduction of its overall cellular levels. The first suggests that the CKX1 oligomerization status may represent an important determinant for its ER retention and, consequently, for the cytokinin concentration and signaling activity in the ER. ER retention mechanisms based on TM-mediated protein dimerization were proposed earlier (e.g. for the type II TM

chaperone COSMS; Sun et al., 2011). It should be noted, however, that the ER residency of membrane proteins often can be determined by the combined activity of different retention and retrieval signals (Boulaflous et al., 2009). Therefore, it will be interesting to analyze whether the ER localization of CKX1 is eventually controlled by additional sorting signals (Cosson et al., 2013; Gao et al., 2014). Second, our analysis demonstrated that plants expressing the monomeric CKX1 mutant variant accumulated the protein to levels considerably lower than those detected in plants expressing the wild-type form. The reduced protein levels were correlated with the lack of a prominent cytokinin deficiency phenotype in the respective transgenic lines, suggesting that the capacity of the mutant protein to regulate the cytokinin concentration in the ER was impaired. Less severe reduction of endogenous cytokinin levels in *35S:CKX1-GFP*-expressing lines corroborated this conclusion. It is interesting that the cytokinin levels in these lines were still significantly lower in comparison with the wild type, which is in line with the notion that the cytokinin signal must be reduced below a certain threshold to trigger strong growth alterations (Werner et al., 2010).

We have recently shown that CKX1 as well as apparently other CKX isoforms targeted to the secretory pathway are regulated by the proteasome-dependent ERAD pathway (Niemann et al., 2015), which represents a conserved cellular route to withdraw proteins from the ER that fail to attain their native conformation (Römisch, 2005). Therefore, it is conceivable that the unassembled monomeric CKX1 is prone to increased degradation by ERAD. Consistent with this hypothesis, the CKX1-GFP protein levels were significantly restored by treatments with ERAD inhibitors, indicating that CKX1 oligomerization is a crucial parameter determining its ERAD and, hence, the protein abundance in the ER. The exact mechanisms underlying ERAD of CKX1 and other CKX proteins are currently unknown; however, it can be hypothesized that the assembly of individual subunits into multimeric complexes can enhance protein folding or conformational stability, which can prevent proteolytic degradation (Vembar and Brodsky, 2008). Although it needs to be studied in more detail, it is interesting that CKX1-GFP levels were not fully rescued by the ERAD inhibition, suggesting that, eventually, other mechanisms may be involved in CKX1 removal from the ER as well.

It should be further noted that detailed genetic studies will be required in the future to complement the data presented here and to identify biological processes involving the molecular mechanisms described in this work.

MATERIALS AND METHODS

Plasmid Construction

The *35S:myc-CKX1* construct was described previously (Niemann et al., 2015). To generate *35S:GFP-CKX1*, the CKX1 cDNA from pDONR221-CKX1 (Niemann et al., 2015) was subcloned into pK7WGF2 (Karimi et al., 2002) by Gateway LR recombination (Invitrogen). For *35S:CKX1-GFP*, the *CKX1* cDNA was PCR amplified in two steps by using primer pairs 1/2 and 3/4 (Supplemental Table S1), and the final amplicon was cloned into the vector pDONR221 (Invitrogen) and subsequently pK7FWG2 (Karimi et al., 2002). The *CKX1$^{1-79}$-GFP* fusion gene was created by overlapping PCR. In the first step, the *CKX1* fragment and GFP-coding sequence were amplified by using primer pairs 3/5 and 6/7 and pDONR221-CKX1 and pK7WGF2 as templates, respectively. These two fragments were combined and amplified with primers 3 and 4, and the final amplicon was cloned successively in pDONR221 and pK7FWG2 to generate *35S:CKX1$^{1-79}$-GFP*. The CKX1-GFP construct was generated by site-directed mutagenesis (Eurofins Genomics).

For protein-protein interaction by BiFC, the *CKX1* cDNA was PCR amplified using primer pairs 8/9 and 10/11, and the resulting fragments were cloned into pJet vector. First, CKX1 cDNA was subcloned into the MCS1 *Bam*HI site of pDOE-08 (Gookin and Assmann, 2014), resulting in pDOE-08-CKX1 parent vector expressing CKX1 N-terminally tagged with the N-terminal fragment of monomeric Venus split at residue 210 (NVen-CKX1) and unfused C-terminal Venus fragment (CVen). This vector was used as a negative control. In the next step, the second CKX1 cDNA fragment was subcloned into the *Kfl*I site within MCS3 of the pDOE-08-CKX1 parent vector, resulting in vector expressing NVen-CKX1/CVen-CKX1 used for the homodimerization test. Mutated full-length *CKX1* cDNA was used in a similar cloning approach to generate the vector encoding NVen-CKX1/CVen-CKX1.

Single-copy transgenic Arabidopsis (*Arabidopsis thaliana*) lines harboring *35S:CKX1-GFP* and *35S:CKX1-GFP* were used in this study.

Transient Expression in *Nicotiana benthamiana* and Confocal Laser Scanning Microscopy

Infiltration was performed as described previously (Sparkes et al., 2006; Niemann et al., 2015) using *Agrobacterium tumefaciens* strain GV3101:pMP90 and 6-week-old *N. benthamiana* plants. For coexpression, the *A. tumefaciens* cultures harboring different expression constructs were mixed in infiltration medium to a final OD_{600} of 0.1 for the CKX1 fusions and 0.01 to 0.05 for the marker constructs. *35S:p19* was included in all infiltrations at OD_{600} = 0.1. The following binary constructs were used in this work: pH7MP:RFP (Boutant et al., 2010), RFP-p24 (Lerich et al., 2011), ERD2-YFP (Brandizzi et al., 2002), YFP-Sec24 (Stefano et al., 2006), mCherry-SYP61 (Gu and Innes, 2011), and ARA6-mCherry (Gu and Innes, 2012). Confocal imaging analysis was performed using a Leica TCS SP5 laser scanning confocal microscope 1 to 3 d after infiltration. mTq2, GFP, YFP, RFP, and mCherry were excited at 458, 488, 514, and 561 nm, and the fluorescence emissions were detected at 461 to 488, 498 to 538, 520 to 556, 600 to 630, and 590 to 640 nm, respectively. In cases where GFP and YFP were analyzed simultaneously, GFP and YFP were detected at 490 to 507 and 557 to 585 nm, respectively.

Preparation of Microsomal Membranes and Membrane Association Analysis

N. benthamiana leaves (1 g) were homogenized in 5 mL of homogenization buffer (25 mM Tris-HCl, pH 7.5, 300 mM Suc, 1 mM EDTA, 1 mM 1,4-dithioerythritol, and complete protease inhibitor cocktail without EDTA [Roche]) using a mortar and pestle. The homogenate was passed through one layer of Miracloth (Calbiochem) and centrifuged at 10,000*g* for 10 min at 4°C to remove the debris. The microsomal membrane fraction was pelleted by ultracentrifugation at 100,000*g* for 90 min at 4°C. Pellets were resuspended in 5 mL of homogenization buffer or homogenization buffer supplemented with 1 M NaCl, 2 M urea, 0.1 M Na_2CO_3, pH 11, or 1% Triton X-100.

For the protease digestion assay, the microsomal membranes were isolated from rosettes of 14-d-old soil-grown Arabidopsis plants expressing *35S:myc-CKX1* (Niemann et al., 2015) and *35S:CKX1-myc*. The 100,000*g* pellet was resuspended in proteinase inhibitor-free homogenization buffer and incubated with 10 $\mu g\ mL^{-1}$ proteinase K at room temperature for 45 min in the presence or absence of 1% Triton X-100. A concentration of 6 mM phenylmethanesulfonyl fluoride (Sigma-Aldrich) was used to terminate the protease digestions. After 15 min of incubation on ice, the membranes were solubilized with 2× SDS-PAGE sample buffer (125 mM Tris-HCl, pH 6.8, 4% SDS, 20% glycerol, 10% β-mercaptoethanol, and 0.01% Bromphenol Blue).

Protein samples were resolved by SDS-PAGE and blotted on PVDF membranes (Millipore). Membranes were blocked with 5% skim milk in PBS containing 0.1% Tween 20. A mouse monoclonal anti-myc antibody (clone 4A6;

Millipore; dilution 1:1,000) followed by a goat anti-mouse antibody coupled to horseradish peroxidase (sc-2005; Santa-Cruz; dilution 1:2,000) were used to detect myc-CKX1. For immunodetection of Arabidopsis calnexins, the blots were stripped (2 × 10 min; 1.5% Gly, 0.1% SDS, and 1% Tween 20, pH 2.2) and reprobed by using anti-CNX1/2 antibody (Agrisera; dilution 1:10,000) and horseradish peroxidase-conjugated goat anti-rabbit antibody (Calbiochem; dilution 1:2,000). Bound antibodies were visualized with SuperSignal West Pico chemiluminescent substrate (Thermo Scientific).

Co-IP Assays

GFP and myc fusion proteins were coexpressed in *N. benthamiana* leaves, which were ground in liquid nitrogen and homogenized in extraction buffer (50 mM Tris-HCl, pH 7.5, 150 mM NaCl, 0.3% Triton X-100, 0.2% Igepal, 1 mM phenylmethanesulfonyl fluoride, and complete protease inhibitor cocktail [Roche]). Samples were cleared by 10 min of centrifugation at 4°C and 6,000*g*. Supernatants (1.4 mL) were adjusted to 2.8 mg mL^{-1} protein and incubated with 20 μL of GFP-Trap-A beads (Chromotek) for 3 to 4 h at 4°C. Beads were washed five times with the extraction buffer, mixed with 20 μL of 2× SDS-PAGE sample buffer, incubated for 5 min at 95°C, and cleared by centrifugation. The proteins were subjected to SDS-PAGE and immunoblot analysis using anti-myc or anti-GFP antibody (clone JL-8; Clontech; dilution 1:2,500).

SEC

Microsomal membranes were isolated according to the protocol by Abas and Luschnig (2010). Briefly, *N. benthamiana* leaves were homogenized in 1 volume of extraction buffer (100 mM Tris-HCl, pH 7.5, 300 mM NaCl, 25% Suc, and 5% glycerol). The homogenate was kept on ice for 20 min and centrifuged at 600*g* for 3 min. After an additional 20 min of incubation on ice, the supernatant was diluted with 1 volume of water, divided into 200-μL aliquots in 1.5-mL tubes, and centrifuged at 16,000*g* for 2.5 h. The membranes from 7 g of leaves were solubilized in 1 volume of buffer (50 mM Tris-HCl, pH 7.5, 150 mM NaCl, 20% glycerol, 15 mM β-mercaptoethanol, and 1% DDM) overnight at 4°C. Membrane proteins were concentrated using Amicon Ultra-15 centrifugal filter units (50-kD cutoff; Millipore). The whole protein extract was loaded on the HiLoad 16/60 Superdex 200 column (GE Healthcare) equilibrated with at least 3 column volumes of running buffer (50 mM Tris-HCl, pH 7.5, 150 mM NaCl, 10% glycerol, and 0.05% DDM). Chromatography was performed with the ÄKTA FPLC system (GE Healthcare) at a flow rate of 1 mL min^{-1}. Elution fractions of 1 mL were collected and subjected to SDS-PAGE followed by western blotting and immunodetection. The Superdex 200 column was calibrated using the following proteins as standards: BSA trimer (201 kD), BSA dimer (132 kD), BSA monomer (67 kD), and ovalbumin (43 kD).

RNA Extraction, cDNA Synthesis, and Quantitative PCR

RNA extraction from shoots of single plants, cDNA synthesis, and quantitative PCR were done as described before using *UBC10* for normalization (Niemann et al., 2015). The primers used for *CKX1* amplification in the quantitative PCR were CKX1-fw (5′-ATGGATCAGGAAACTGGCAA-3′) and CKX1-rev (5′-AGATGAAAACAAAGTGGATGGAA-3′).

Treatments with ERAD Inhibitors

Seedlings were grown in liquid cultures for 7 d followed by 24 h of treatment with 50 μM Kif dissolved in water, 20 μM EerI dissolved in DMSO, and the respective mocks. A total of 50 μg of protein extracts was analyzed by immunoblot analysis using anti-GFP antibody as described above. Loading was verified by Coomassie Blue staining after immunoblot detection according to Welinder and Ekblad (2011).

Determination of Cytokinin Content

The cytokinin content in shoots of 3-week-old soil-grown plants was determined by ultra-performance liquid chromatography-electrospray-tandem mass spectrometry as described by Svačinová et al. (2012), including modifications described by Antoniadi et al. (2015).

Computational Modeling

The structure of CKX1-TM was predicted from its sequence (11-RQNNKTFLGIFMILVLSCIAGRTNLCS-37) using CATM (Mueller et al., 2014). Side chain mobility was modeled using the energy-based conformer library applied at the 95% level (Subramaniam and Senes, 2012). Energies were determined using the CHARMM 22 van der Waals function (MacKerell et al., 1998) and the hydrogen bonding function of SCWRL 4 (Krivov et al., 2009), as implemented in MSL (Kulp et al., 2012), with the following parameters for Cα donors, as reported previously: B = 60.278; D_0 = 2.3 Å; σ_d = 1.202 Å; α_{max} = 74°; and β_{max} = 98° (Mueller et al., 2014). The relative energy of the Ser-27Ile, Gly-31Ile mutant was calculated as

$$\Delta E_{mut} = \left(E_{mut,dimer} - E_{mut,monomer}\right) - \left(E_{WT,dimer} - E_{WT,monomer}\right)$$

where $E_{WT,dimer}$ and $E_{mut,dimer}$ are the energies of the wild-type and mutant sequences, respectively, in the dimeric state and $E_{WT,monomer}$ and $E_{mut,monomer}$ are the energies of the wild-type and mutant sequences, respectively, in a side chain-optimized monomeric state with the same sequence.

Accession Numbers

Sequence data from this article can be found in the GenBank/EMBL data libraries under accession number At2G41510 (*CKX1*).

Supplemental Data

The following supplemental materials are available.

Supplemental Figure S1. Co-IP detection of CKX1 oligomerization.

Supplemental Figure S2. SEC analysis of CKX1 complex formation.

Supplemental Figure S3. Strong overexpression of GFP-CKX1 alters the ER morphology.

Supplemental Figure S4. Co-IP detection of homooligomerization mediated by the CKX11-79 N-terminal fragment.

Supplemental Figure S5. CKX1-TM-GFP is *N*-glycosylated and membrane associated.

Supplemental Figure S6. Structural model of the Ser-27Ile, Gly-31Ile double mutant of CKX1.

Supplemental Figure S7. Growth and molecular phenotypes of Arabidopsis plants expressing 35S:CKX1-GFP and 35S:CKX1-TM-GFP.

Supplemental Table S1. Oligonucleotides used in this study.

ACKNOWLEDGMENTS

We thank Roger Innes for providing the mCherry-SYP61 and ARA6-mCherry constructs, Manfred Heinlein for the MP:RFP construct, and Federica Brandizzi for the ERD2-YFP and YFP-Sec24 constructs. We thank Sören Werner and Thomas Schmülling for providing the 35S:CKX1-myc construct.

Received July 10, 2017; accepted December 29, 2017; published January 4, 2018.

LITERATURE CITED

Abas L, Luschnig C (2010) Maximum yields of microsomal-type membranes from small amounts of plant material without requiring ultracentrifugation. Anal Biochem **401:** 217–227

Anderson SM, Mueller BK, Lange EJ, Senes A (2017) Combination of Cα-H hydrogen bonds and van der Waals packing modulates the stability of GxxxG-mediated dimers in membranes. J Am Chem Soc **139:** 15774–15783

Antoniadi I, Plačková L, Simonovik B, Doležal K, Turnbull C, Ljung K, Novák O (2015) Cell-type-specific cytokinin distribution within the *Arabidopsis* primary root apex. Plant Cell **27:** 1955–1967

Barrieu F, Chrispeels MJ (1999) Delivery of a secreted soluble protein to the vacuole via a membrane anchor. Plant Physiol **120:** 961–968

Bartrina I, Otto E, Strnad M, Werner T, Schmülling T (2011) Cytokinin regulates the activity of reproductive meristems, flower organ size, ovule formation, and thus seed yield in *Arabidopsis thaliana*. Plant Cell **23:** 69–80

Bi G, Liebrand TWH, Bye RR, Postma J, van der Burgh AM, Robatzek S, Xu X, Joosten MHAJ (2016) SOBIR1 requires the GxxxG dimerization motif in its transmembrane domain to form constitutive complexes with receptor-like proteins. Mol Plant Pathol **17:** 96–107

Bilyeu KD, Cole JL, Laskey JG, Riekhof WR, Esparza TJ, Kramer MD, Morris RO (2001) Molecular and biochemical characterization of a cytokinin oxidase from maize. Plant Physiol **125:** 378–386

Boulaflous A, Saint-Jore-Dupas C, Herranz-Gordo MC, Pagny-Salehabadi S, Plasson C, Garidou F, Kiefer-Meyer MC, Ritzenthaler C, Faye L, Gomord V (2009) Cytosolic N-terminal arginine-based signals together with a luminal signal target a type II membrane protein to the plant ER. BMC Plant Biol **9:** 144

Boutant E, Didier P, Niehl A, Mély Y, Ritzenthaler C, Heinlein M (2010) Fluorescent protein recruitment assay for demonstration and analysis of in vivo protein interactions in plant cells and its application to Tobacco mosaic virus movement protein. Plant J **62:** 171–177

Brandizzi F, Frangne N, Marc-Martin S, Hawes C, Neuhaus JM, Paris N (2002) The destination for single-pass membrane proteins is influenced markedly by the length of the hydrophobic domain. Plant Cell **14:** 1077–1092

Caesar K, Thamm AMK, Witthöft J, Elgass K, Huppenberger P, Grefen C, Horak J, Harter K (2011) Evidence for the localization of the *Arabidopsis* cytokinin receptors AHK3 and AHK4 in the endoplasmic reticulum. J Exp Bot **62:** 5571–5580

Chevalier AS, Chaumont F (2015) Trafficking of plant plasma membrane aquaporins: multiple regulation levels and complex sorting signals. Plant Cell Physiol **56:** 819–829

Choma C, Gratkowski H, Lear JD, DeGrado WF (2000) Asparagine-mediated self-association of a model transmembrane helix. Nat Struct Biol **7:** 161–166

Chung KM, Cheng JH, Suen CS, Huang CH, Tsai CH, Huang LH, Chen YR, Wang AHJ, Jiaang WT, Hwang MJ, et al (2010) The dimeric transmembrane domain of prolyl dipeptidase DPP-IV contributes to its quaternary structure and enzymatic activities. Protein Sci **19:** 1627–1638

Cosson P, Perrin J, Bonifacino JS (2013) Anchors aweigh: protein localization and transport mediated by transmembrane domains. Trends Cell Biol **23:** 511–517

De Marcos Lousa C, Gershlick DC, Denecke J (2012) Mechanisms and concepts paving the way towards a complete transport cycle of plant vacuolar sorting receptors. Plant Cell **24:** 1714–1732

Dews IC, Mackenzie KR (2007) Transmembrane domains of the syndecan family of growth factor coreceptors display a hierarchy of homotypic and heterotypic interactions. Proc Natl Acad Sci USA **104:** 20782–20787

Fiebiger E, Hirsch C, Vyas JM, Gordon E, Ploegh HL, Tortorella D (2004) Dissection of the dislocation pathway for type I membrane proteins with a new small molecule inhibitor, eeyarestatin. Mol Biol Cell **15:** 1635–1646

Fritz-Laylin LK, Krishnamurthy N, Tör M, Sjölander KV, Jones JDG (2005) Phylogenomic analysis of the receptor-like proteins of rice and Arabidopsis. Plant Physiol **138:** 611–623

Fujiki Y, Hubbard AL, Fowler S, Lazarow PB (1982) Isolation of intracellular membranes by means of sodium carbonate treatment: application to endoplasmic reticulum. J Cell Biol **93:** 97–102

Fusseder A, Ziegler P (1988) Metabolism and compartmentation of dihydrozeatin exogenously supplied to photoautotrophic suspension cultures of *Chenopodium rubrum*. Planta **173:** 104–109

Galuszka P, Frébortová J, Luhová L, Bilyeu KD, English JT, Frébort I (2005) Tissue localization of cytokinin dehydrogenase in maize: possible involvement of quinone species generated from plant phenolics by other enzymatic systems in the catalytic reaction. Plant Cell Physiol **46:** 716–728

Galuszka P, Popelková H, Werner T, Frébortová J, Pospísilová H, Mik V, Köllmer I, Schmülling T, Frébort I (2007) Biochemical characterization of cytokinin oxidases/dehydrogenases from *Arabidopsis thaliana* expressed in *Nicotiana tabacum* L. J Plant Growth Regul **26:** 255–267

Gao C, Cai Y, Wang Y, Kang BH, Aniento F, Robinson DG, Jiang L (2014) Retention mechanisms for ER and Golgi membrane proteins. Trends Plant Sci **19:** 508–515

Gimpelev M, Forrest LR, Murray D, Honig B (2004) Helical packing patterns in membrane and soluble proteins. Biophys J **87:** 4075–4086

Gookin TE, Assmann SM (2014) Significant reduction of BiFC non-specific assembly facilitates *in planta* assessment of heterotrimeric G-protein interactors. Plant J **80:** 553–567

Gu Y, Innes RW (2011) The KEEP ON GOING protein of Arabidopsis recruits the ENHANCED DISEASE RESISTANCE1 protein to *trans*-Golgi network/early endosome vesicles. Plant Physiol **155:** 1827–1838

Gu Y, Innes RW (2012) The KEEP ON GOING protein of *Arabidopsis* regulates intracellular protein trafficking and is degraded during fungal infection. Plant Cell **24:** 4717–4730

Hanton SL, Matheson LA, Brandizzi F (2006) Seeking a way out: export of proteins from the plant endoplasmic reticulum. Trends Plant Sci **11:** 335–343

Hoang T, Kuljanin M, Smith MD, Jelokhani-Niaraki M (2015) A biophysical study on molecular physiology of the uncoupling proteins of the central nervous system. Biosci Rep **35:** e00226

Holst K, Schmülling T, Werner T (2011) Enhanced cytokinin degradation in leaf primordia of transgenic *Arabidopsis* plants reduces leaf size and shoot organ primordia formation. J Plant Physiol **168:** 1328–1334

Houba-Hérin N, Pethe C, d'Alayer J, Laloue M (1999) Cytokinin oxidase from Zea mays: purification, cDNA cloning and expression in moss protoplasts. Plant J **17:** 615–626

Huang L, Franklin AE, Hoffman NE (1993) Primary structure and characterization of an *Arabidopsis thaliana* calnexin-like protein. J Biol Chem **268:** 6560–6566

Hwang I, Sheen J, Müller B (2012) Cytokinin signaling networks. Annu Rev Plant Biol **63:** 353–380

Inoue T, Higuchi M, Hashimoto Y, Seki M, Kobayashi M, Kato T, Tabata S, Shinozaki K, Kakimoto T (2001) Identification of CRE1 as a cytokinin receptor from *Arabidopsis*. Nature **409:** 1060–1063

Jiskrová E, Novák O, Pospíšilová H, Holubová K, Karády M, Galuszka P, Robert S, Frébort I (2016) Extra- and intracellular distribution of cytokinins in the leaves of monocots and dicots. N Biotechnol **33:** 735–742

Johnson RM, Hecht K, Deber CM (2007) Aromatic and cation-π interactions enhance helix-helix association in a membrane environment. Biochemistry **46:** 9208–9214

Jürgens G (2004) Membrane trafficking in plants. Annu Rev Cell Dev Biol **20:** 481–504

Karimi M, Inzé D, Depicker A (2002) GATEWAY vectors for *Agrobacterium*-mediated plant transformation. Trends Plant Sci **7:** 193–195

Kiran NS, Benková E, Reková A, Dubová J, Malbeck J, Palme K, Brzobohatý B (2012) Retargeting a maize β-glucosidase to the vacuole: evidence from intact plants that zeatin-*O*-glucoside is stored in the vacuole. Phytochemistry **79:** 67–77

Köllmer I, Novák O, Strnad M, Schmülling T, Werner T (2014) Overexpression of the cytosolic cytokinin oxidase/dehydrogenase (CKX7) from Arabidopsis causes specific changes in root growth and xylem differentiation. Plant J **78:** 359–371

Kowalska M, Galuszka P, Frébortová J, Šebela M, Béres T, Hluska T, Šmehilová M, Bilyeu KD, Frébort I (2010) Vacuolar and cytosolic cytokinin dehydrogenases of *Arabidopsis thaliana*: heterologous expression, purification and properties. Phytochemistry **71:** 1970–1978

Krivov GG, Shapovalov MV, Dunbrack RL Jr (2009) Improved prediction of protein side-chain conformations with SCWRL4. Proteins **77:** 778–795

Kulp DW, Subramaniam S, Donald JE, Hannigan BT, Mueller BK, Grigoryan G, Senes A (2012) Structural informatics, modeling, and design with an open-source Molecular Software Library (MSL). J Comput Chem **33:** 1645–1661

Kunji ER, Harding M, Butler PJ, Akamine P (2008) Determination of the molecular mass and dimensions of membrane proteins by size exclusion chromatography. Methods **46:** 62–72

Kwon MJ, Choi Y, Yun JH, Lee W, Han IO, Oh ES (2015) A unique phenylalanine in the transmembrane domain strengthens homodimerization of the syndecan-2 transmembrane domain and functionally regulates syndecan-2. J Biol Chem **290:** 5772–5782

Langhans M, Marcote MJ, Pimpl P, Virgili-López G, Robinson DG, Aniento F (2008) *In vivo* trafficking and localization of p24 proteins in plant cells. Traffic **9:** 770–785

Lerich A, Langhans M, Sturm S, Robinson DG (2011) Is the 6 kDa tobacco etch viral protein a bona fide ERES marker? J Exp Bot **62:** 5013–5023

Li E, Hristova K (2006) Role of receptor tyrosine kinase transmembrane domains in cell signaling and human pathologies. Biochemistry **45:** 6241–6251

Li E, Wimley WC, Hristova K (2012) Transmembrane helix dimerization: beyond the search for sequence motifs. Biochim Biophys Acta **1818:** 183–193

Lomin SN, Yonekura-Sakakibara K, Romanov GA, Sakakibara H (2011) Ligand-binding properties and subcellular localization of maize cytokinin receptors. J Exp Bot **62:** 5149–5159

MacKenzie KR, Prestegard JH, Engelman DM (1997) A transmembrane helix dimer: structure and implications. Science **276:** 131–133

MacKerell AD, Bashford D, Bellott M, Dunbrack RL, Evanseck JD, Field MJ, Fischer S, Gao J, Guo H, Ha S, et al (1998) All-atom empirical potential for molecular modeling and dynamics studies of proteins. J Phys Chem B **102:** 3586–3616

Maruyama IN (2015) Activation of transmembrane cell-surface receptors via a common mechanism? The "rotation model." BioEssays **37:** 959–967

Miyawaki A, Sawano A, Kogure T (2003) Lighting up cells: labelling proteins with fluorophores. Nat Cell Biol (Suppl) S1–S7

Moore DT, Berger BW, DeGrado WF (2008) Protein-protein interactions in the membrane: sequence, structural, and biological motifs. Structure **16:** 991–1001

Mothes W, Heinrich SU, Graf R, Nilsson I, von Heijne G, Brunner J, Rapoport TA (1997) Molecular mechanism of membrane protein integration into the endoplasmic reticulum. Cell **89:** 523–533

Mueller BK, Subramaniam S, Senes A (2014) A frequent, GxxxG-mediated, transmembrane association motif is optimized for the formation of interhelical Cα-H hydrogen bonds. Proc Natl Acad Sci USA **111:** E888–E895

Niehl A, Amari K, Gereige D, Brandner K, Mély Y, Heinlein M (2012) Control of *Tobacco mosaic virus* movement protein fate by CELL-DIVISION-CYCLE protein48. Plant Physiol **160:** 2093–2108

Niemann MCE, Bartrina I, Ashikov A, Weber H, Novák O, Spíchal L, Strnad M, Strasser R, Bakker H, Schmülling T, et al (2015) *Arabidopsis* ROCK1 transports UDP-GlcNAc/UDP-GalNAc and regulates ER protein quality control and cytokinin activity. Proc Natl Acad Sci USA **112:** 291–296

Obrdlik P, Neuhaus G, Merkle T (2000) Plant heterotrimeric G protein β subunit is associated with membranes via protein interactions involving coiled-coil formation. FEBS Lett **476:** 208–212

Petersen TN, Brunak S, von Heijne G, Nielsen H (2011) SignalP 4.0: discriminating signal peptides from transmembrane regions. Nat Methods **8:** 785–786

Rögner M (2000) Size exclusion chromatography. *In* M Kastner, ed, Journal of Chromatography Library, Vol 61. Elsevier, Amsterdam pp 89–145

Rojo E, Denecke J (2008) What is moving in the secretory pathway of plants? Plant Physiol **147:** 1493–1503

Römisch K (2005) Endoplasmic reticulum-associated degradation. Annu Rev Cell Dev Biol **21:** 435–456

Russ WP, Engelman DM (2000) The GxxxG motif: a framework for transmembrane helix-helix association. J Mol Biol **296:** 911–919

Sambade A, Brandner K, Hofmann C, Seemanpillai M, Mutterer J, Heinlein M (2008) Transport of TMV movement protein particles associated with the targeting of RNA to plasmodesmata. Traffic **9:** 2073–2088

Schekman R, Orci L (1996) Coat proteins and vesicle budding. Science **271:** 1526–1533

Schmülling T, Werner T, Riefler M, Krupková E, Bartrina y Manns I (2003) Structure and function of cytokinin oxidase/dehydrogenase genes of maize, rice, *Arabidopsis* and other species. J Plant Res **116:** 241–252

Schook W, Puszkin S, Bloom W, Ores C, Kochwa S (1979) Mechanochemical properties of brain clathrin: interactions with actin and alpha-actinin and polymerization into basketlike structures or filaments. Proc Natl Acad Sci USA **76:** 116–120

Schwacke R, Schneider A, van der Graaff E, Fischer K, Catoni E, Desimone M, Frommer WB, Flügge UI, Kunze R (2003) ARAMEMNON, a novel database for Arabidopsis integral membrane proteins. Plant Physiol **131:** 16–26

Senes A, Engel DE, DeGrado WF (2004) Folding of helical membrane proteins: the role of polar, GxxxG-like and proline motifs. Curr Opin Struct Biol **14:** 465–479

Senes A, Gerstein M, Engelman DM (2000) Statistical analysis of amino acid patterns in transmembrane helices: the GxxxG motif occurs frequently and in association with β-branched residues at neighboring positions. J Mol Biol **296:** 921–936

Senes A, Ubarretxena-Belandia I, Engelman DM (2001) The Calpha—H... O hydrogen bond: a determinant of stability and specificity in transmembrane helix interactions. Proc Natl Acad Sci USA **98:** 9056–9061

Sparkes IA, Runions J, Kearns A, Hawes C (2006) Rapid, transient expression of fluorescent fusion proteins in tobacco plants and generation of stably transformed plants. Nat Protoc **1:** 2019–2025

Stefano G, Renna L, Chatre L, Hanton SL, Moreau P, Hawes C, Brandizzi F (2006) In tobacco leaf epidermal cells, the integrity of protein export from the endoplasmic reticulum and of ER export sites depends on active COPI machinery. Plant J **46:** 95–110

Subramaniam S, Senes A (2012) An energy-based conformer library for side chain optimization: improved prediction and adjustable sampling. Proteins **80:** 2218–2234

Sun Q, Ju T, Cummings RD (2011) The transmembrane domain of the molecular chaperone Cosmc directs its localization to the endoplasmic reticulum. J Biol Chem **286:** 11529–11542

Suzuki T, Miwa K, Ishikawa K, Yamada H, Aiba H, Mizuno T (2001) The *Arabidopsis* sensor His-kinase, AHk4, can respond to cytokinins. Plant Cell Physiol **42:** 107–113

Svačinová J, Novák O, Plačková L, Lenobel R, Holík J, Strnad M, Doležal K (2012) A new approach for cytokinin isolation from Arabidopsis tissues using miniaturized purification: pipette tip solid-phase extraction. Plant Methods **8:** 17

Tokunaga F, Brostrom C, Koide T, Arvan P (2000) Endoplasmic reticulum (ER)-associated degradation of misfolded N-linked glycoproteins is suppressed upon inhibition of ER mannosidase I. J Biol Chem **275:** 40757–40764

Tu L, Banfield DK (2010) Localization of Golgi-resident glycosyltransferases. Cell Mol Life Sci **67:** 29–41

Ueda T, Yamaguchi M, Uchimiya H, Nakano A (2001) Ara6, a plant-unique novel type Rab GTPase, functions in the endocytic pathway of *Arabidopsis thaliana*. EMBO J **20:** 4730–4741

Uemura T, Ueda T, Ohniwa RL, Nakano A, Takeyasu K, Sato MH (2004) Systematic analysis of SNARE molecules in *Arabidopsis*: dissection of the post-Golgi network in plant cells. Cell Struct Funct **29:** 49–65

van Anken E, Braakman I (2005) Versatility of the endoplasmic reticulum protein folding factory. Crit Rev Biochem Mol Biol **40:** 191–228

Vembar SS, Brodsky JL (2008) One step at a time: endoplasmic reticulum-associated degradation. Nat Rev Mol Cell Biol **9:** 944–957

von Heijne G, Gavel Y (1988) Topogenic signals in integral membrane proteins. Eur J Biochem **174:** 671–678

von Schaewen A, Sturm A, O'Neill J, Chrispeels MJ (1993) Isolation of a mutant *Arabidopsis* plant that lacks *N*-acetyl glucosaminyl transferase I and is unable to synthesize Golgi-modified complex *N*-linked glycans. Plant Physiol **102:** 1109–1118

Walters RFS, DeGrado WF (2006) Helix-packing motifs in membrane proteins. Proc Natl Acad Sci USA **103:** 13658–13663

Wang Q, Shinkre BA, Lee JG, Weniger MA, Liu Y, Chen W, Wiestner A, Trenkle WC, Ye Y (2010) The ERAD inhibitor Eeyarestatin I is a bifunctional compound with a membrane-binding domain and a p97/VCP inhibitory group. PLoS ONE **5:** e15479

Welinder C, Ekblad L (2011) Coomassie staining as loading control in Western blot analysis. J Proteome Res **10:** 1416–1419

Werner T, Motyka V, Laucou V, Smets R, Van Onckelen H, Schmülling T (2003) Cytokinin-deficient transgenic *Arabidopsis* plants show multiple developmental alterations indicating opposite functions of cytokinins in the regulation of shoot and root meristem activity. Plant Cell **15:** 2532–2550

Werner T, Motyka V, Strnad M, Schmülling T (2001) Regulation of plant growth by cytokinin. Proc Natl Acad Sci USA **98:** 10487–10492

Werner T, Nehnevajova E, Köllmer I, Novák O, Strnad M, Krämer U, Schmülling T (2010) Root-specific reduction of cytokinin causes enhanced root growth, drought tolerance, and leaf mineral enrichment in *Arabidopsis* and tobacco. Plant Cell **22:** 3905–3920

Werner T, Schmülling T (2009) Cytokinin action in plant development. Curr Opin Plant Biol **12:** 527–538

Wulfetange K, Lomin SN, Romanov GA, Stolz A, Heyl A, Schmülling T (2011) The cytokinin receptors of Arabidopsis are located mainly to the endoplasmic reticulum. Plant Physiol **156:** 1808–1818

Xu J, Peng H, Chen Q, Liu Y, Dong Z, Zhang JT (2007) Oligomerization domain of the multidrug resistance-associated transporter ABCG2 and its dominant inhibitory activity. Cancer Res **67:** 4373–4381

Zhang Y, Yang Y, Fang B, Gannon P, Ding P, Li X, Zhang Y (2010) *Arabidopsis snc2-1D* activates receptor-like protein-mediated immunity transduced through WRKY70. Plant Cell **22:** 3153–3163

Zhou FX, Cocco MJ, Russ WP, Brunger AT, Engelman DM (2000) Interhelical hydrogen bonding drives strong interactions in membrane proteins. Nat Struct Biol **7:** 154–160